

Supporting Information

Intrinsically Stretchable and Printable Lithium-Ion Battery for Free-Form Configuration

Soo Yeong Hong[†], Sung Min Jee[†], Youngpyo Ko^{†,‡}, Jinhan Cho^{‡,§}, Keun Hyung Lee[‡], Bongjun Yeom[¶], Heesuk Kim[†], Jeong Gon Son^{†,‡}*

[†]Soft Hybrid Materials Research Center, Korea Institute of Science and Technology, Seoul, 02792, Republic of Korea

[‡]KU-KIST Graduate School of Converging Science and Technology, Korea University, Seoul, 02841, Republic of Korea

[§]Department of Chemical and Biological Engineering, Korea University, Seoul, 02841, Republic of Korea

[‡]Department of Chemistry and Chemical Engineering, Inha University, Incheon, 22212, Republic of Korea

[¶]Department of Chemical Engineering, Hanyang University, Seongdong-gu, Seoul 04763, Republic of Korea

* Corresponding author. Email: jgson@kist.re.kr (J. G. Son)

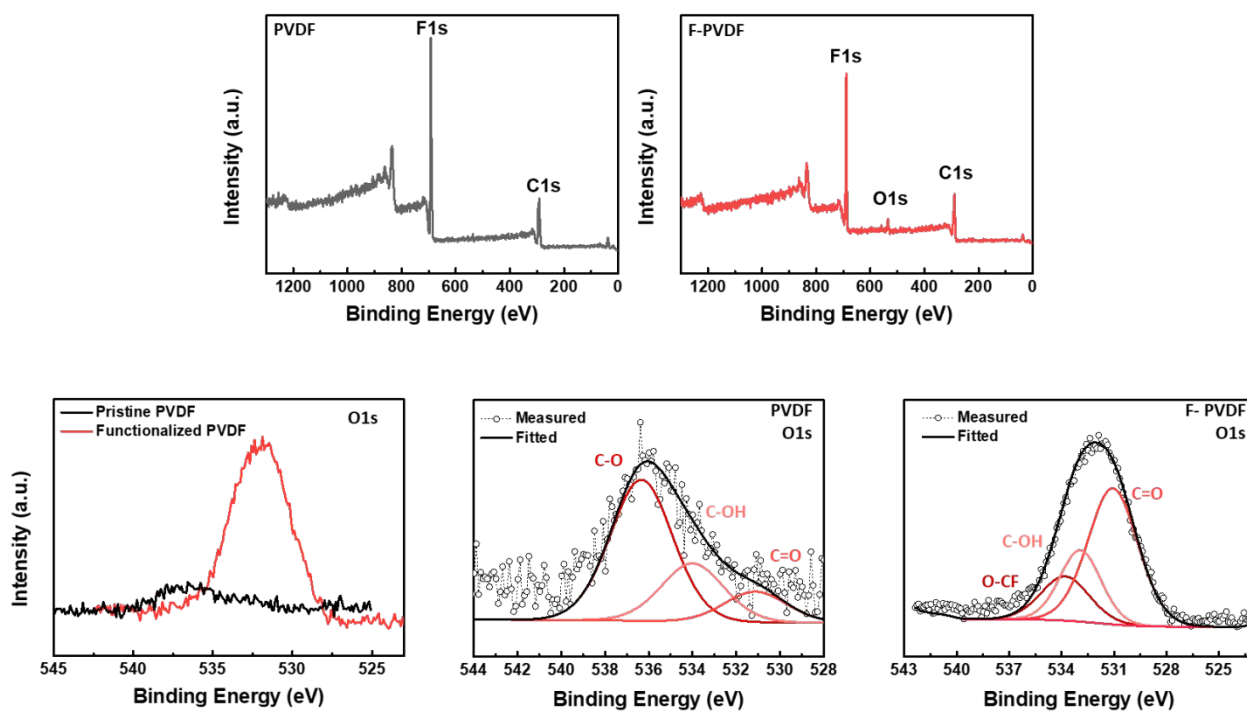


Figure S1. XPS spectra of pristine PVDF and F-PVDF (a) elemental survey (b) O 1s core electron spectra.

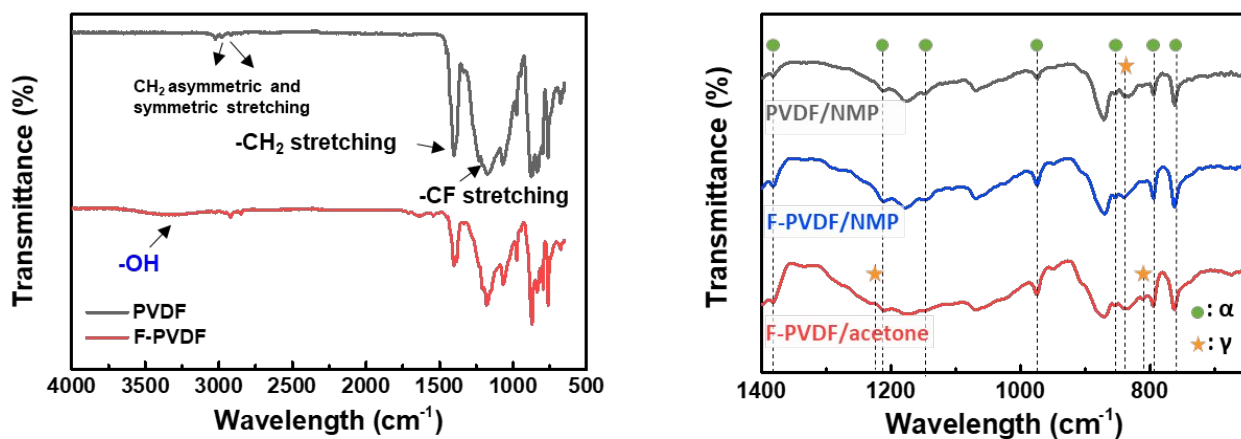


Figure S2. FT-IR spectra of (a) pristine PVDF and F-PVDF powder and (b) PVDF/NMP (gray), F-PVDF/NMP (blue), and F-PVDF/acetone (red) film.

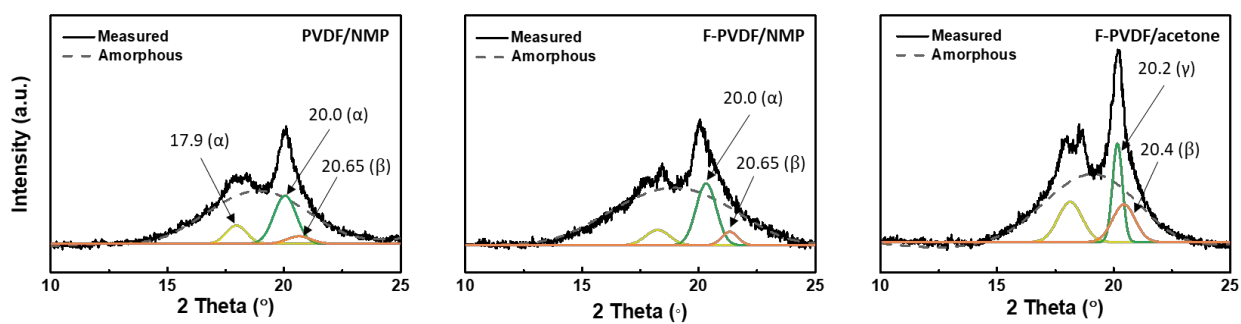


Figure S3. Deconvolution of XRD spectra of pristine PVDF/NMP, F-PVDF/NMP, and F-PVDF/acetone.

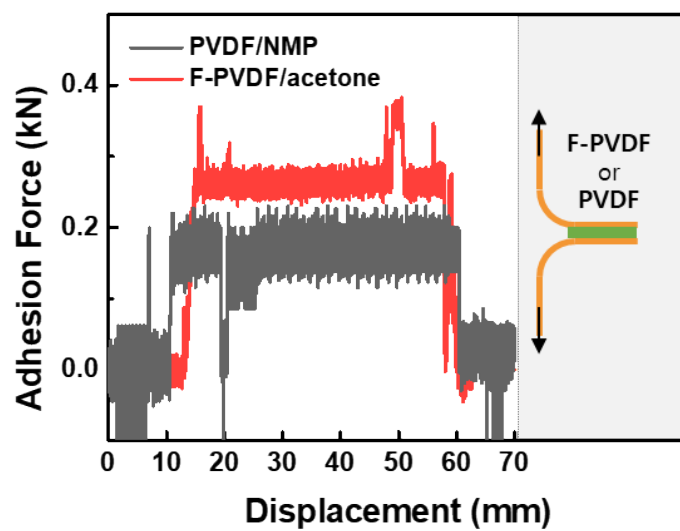


Figure S4. Adhesion force measurements *via* peel testing of the dried PVDF film from NMP and dried F-PVDF film from acetone while immersed in electrolyte.

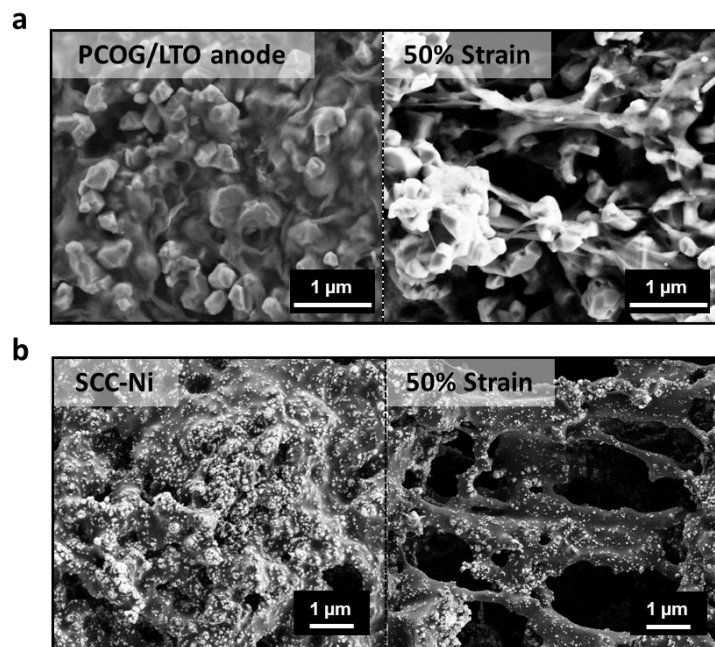


Figure S5. SEM images of the stretchable (a) PCOG/LTO composite anode and (b) SCC-Ni composite at unstained and 50% strained states.

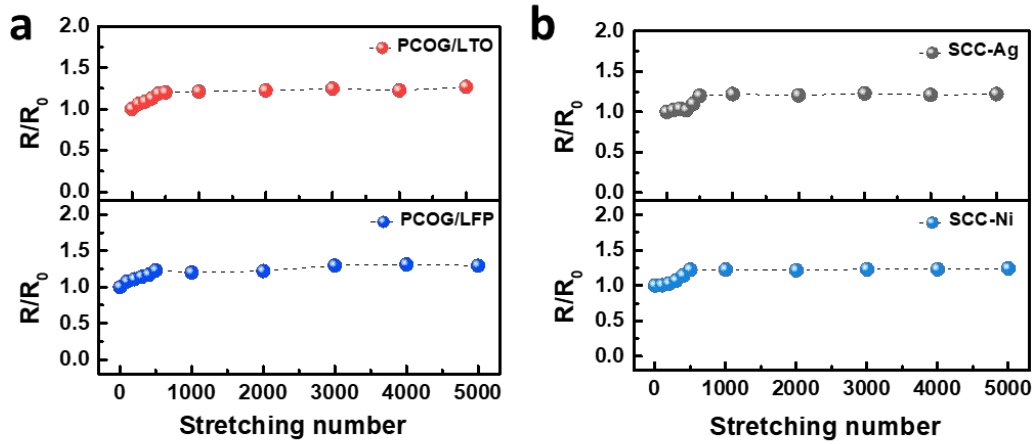


Figure S6. The resistance retention of the (a) PCOG/LTO and PCOG/LFP composite electrodes and (b) SCC-Ag and SCC-Ni composited current collectors as function of repetitive stretching/releasing cycles at 50% strain.

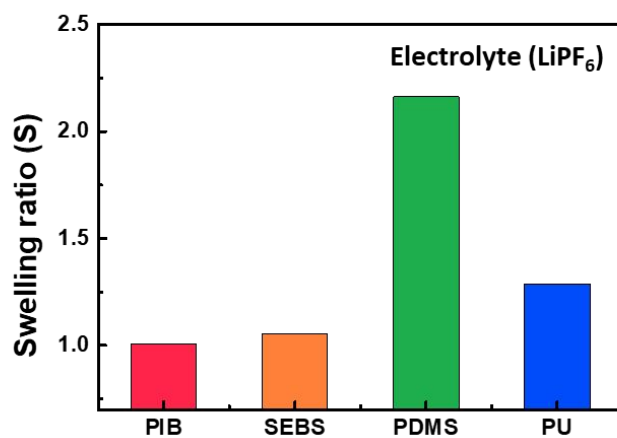


Figure S7. Swelling ratio measurement of PIB, SEBS, PDMS, and PU under saturated vapor of 6M LiPF_6 electrolyte in 1:1:1 EC:DMC:DEC carbonate mixture solvents. The thickness changes of films the films *in-situ* measured by Filmetrics F20 in sealed chamber (9.5 ml) with quartz lid.

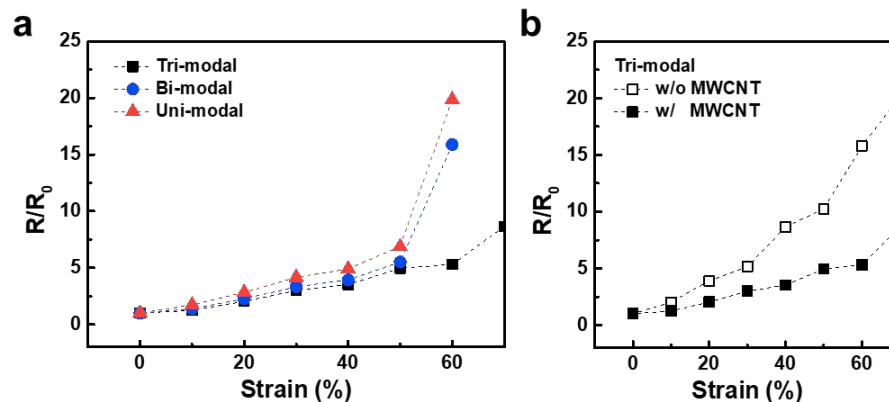


Figure S8. (a) Resistance changes *versus* strain curves of the SCC-Ag composites. In this study, the Ag particles of three different sizes were used to determine the effect of their sizes on the electrical conductivity and stability: (1) Ag nanoparticles smaller than 150 nm (Ag nano), (2) Ag microparticles with a size of 2 - 3.5 μm (Ag microA), and (3) Ag microparticles with a size of 5 - 8 μm (Ag microB). In case of unimodal system, only Ag microB was used, while the mixture of Ag nano and Ag microB in a weight ratio of 4:6 was utilized for bimodal system. The trimodal Ag system is a mixture of Ag Nano, Ag microA and microB in a weight ratio of 2:3:5. (b) Resistance changes *versus* strain curves of the SCC-Ag composites with and without 0.2 wt% of multiwalled carbon nanotubes.



Figure S9. Photographs of the stretchable gel electrolyte based PVDF-HFP PCOG films without and with strain.

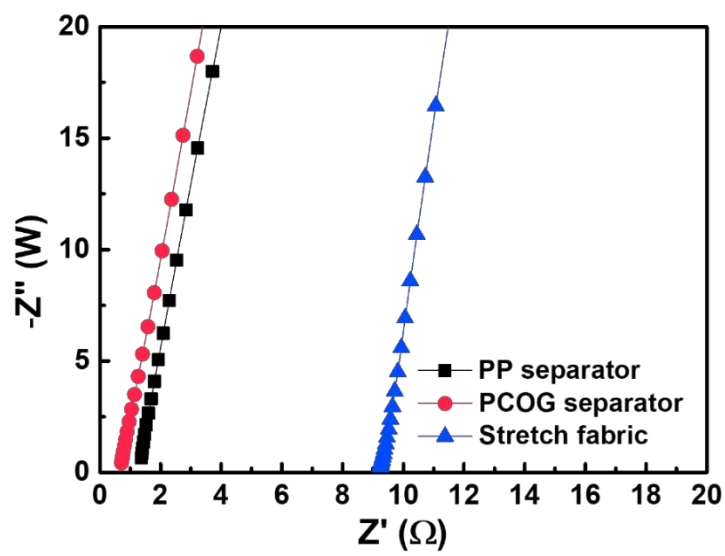


Figure S10. Nyquist plots and bulk resistances of the cell (stainless steel/separator/stainless steel) for 1 M LiPF_6 electrolyte soaked Celgard 2400 (PP, black, 1.4 Ω), PCOG separators (red, 0.8 Ω) and stretch fabric (blue, 9.2 Ω).

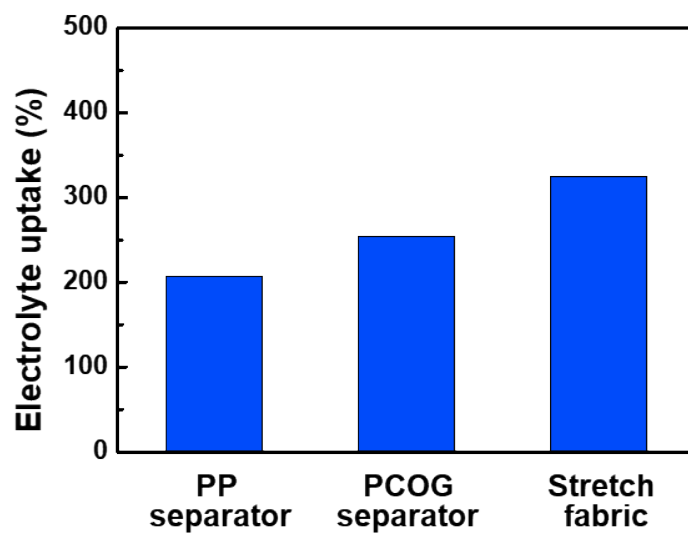


Figure S11. Comparison of electrolyte uptake by PP separator, PCOG separator, and stretch fabric.

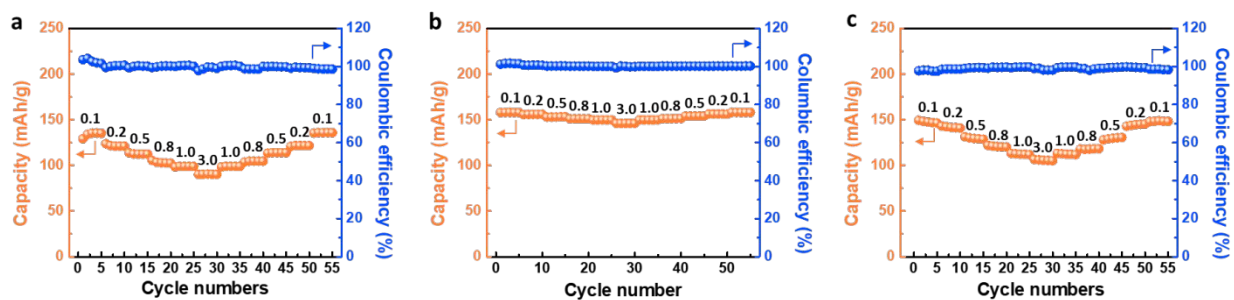


Figure S12. Rate performance and Coulombic efficiencies of (a) PCOG/LFP, (b) PCOG/LTO, and (c) full cell.

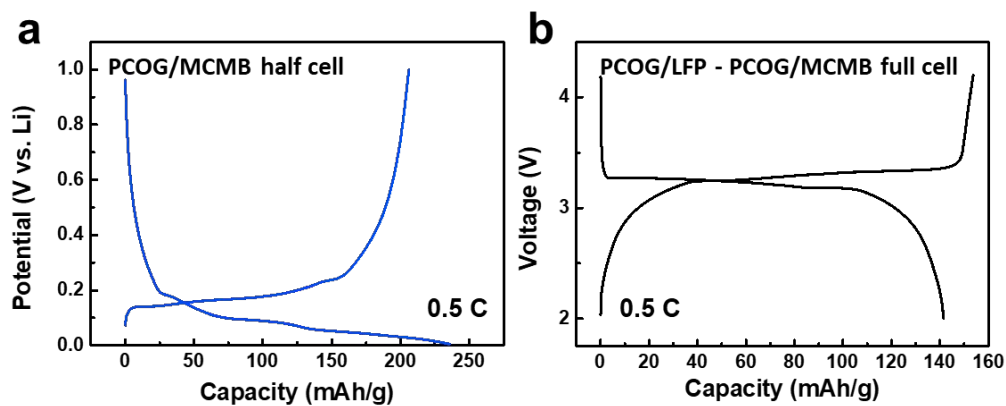


Figure S13. Electrochemical charge/discharge curves of (a) PCOG/MCMB(mesocarbon microbeads) anode (same weight ratio with PCOG/LTO electrode) with half-cell configuration with lithium metal electrode at 0.5 C and (b) PCOG/LFP and PCOG/MCMB full cell between 2 and 4.2 V at 0.5 C with 1 M LiPF_6 in EC/DEC/DMC electrolyte.

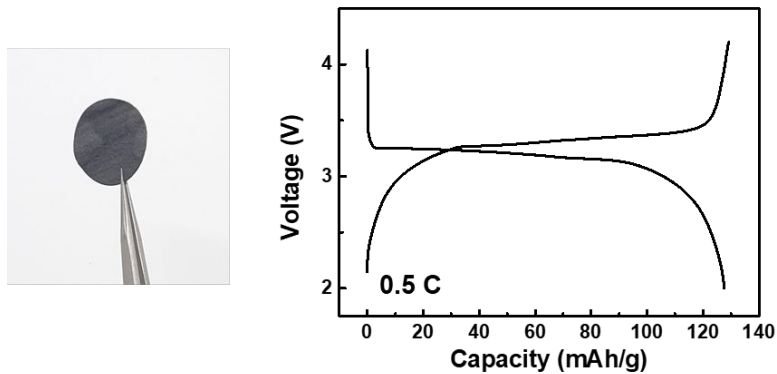


Figure S14. Photographic image of a new ionic liquid (1-Ethyl-3-methylimidazolium bis(trifluoromethylsulfonyl)imide ([EMIM][TFSI])) containing physically crosslinked ion-gels (PCIG)/LFP composite cathode and its electrochemical performance of LIB full cell with a PCIG/MCMB anode and LiTFSI/[EMIM][TFSI] (1:1 weight ratio) electrolyte at 0.5 C.

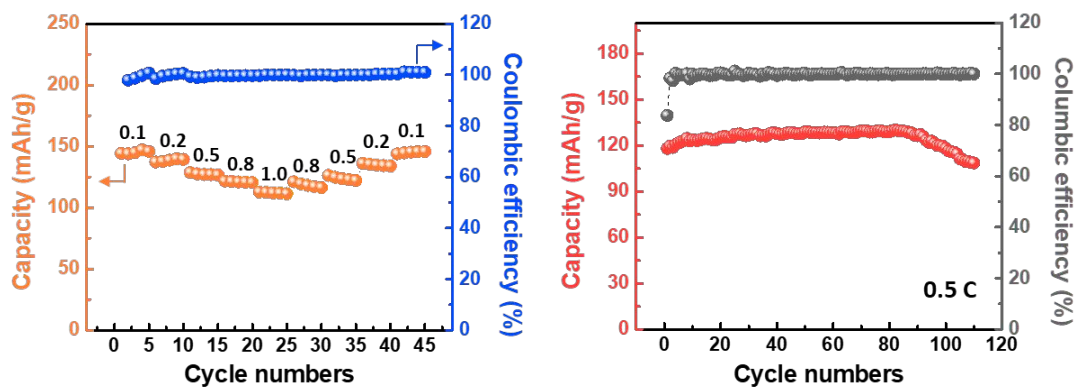


Figure S15. Rate performance, cycling performance and Coulombic efficiency of fully stretchable LIB full cell with stretchable encapsulation.

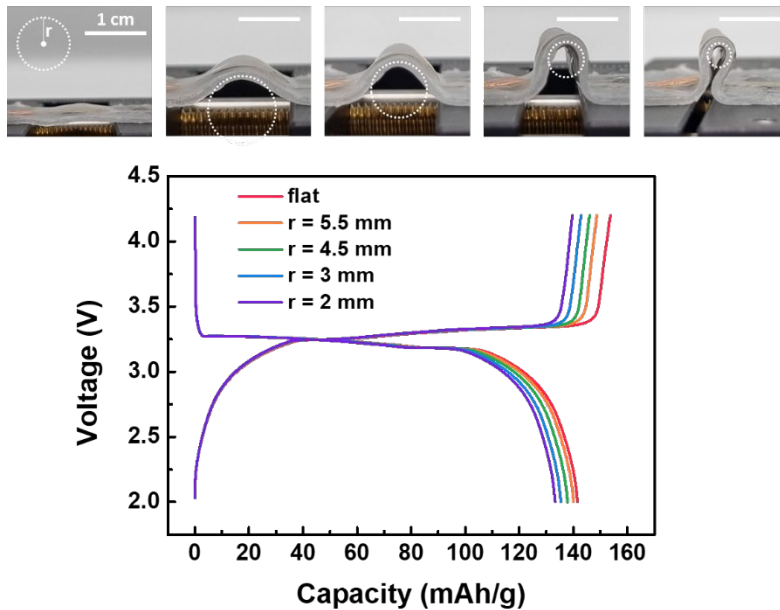


Figure S16. Photographic image of stretchable LIB full cells with PCOG/LFP cathode and PCOG/MCMB anode under the various bending conditions and its electrochemical performances at 0.5 C.

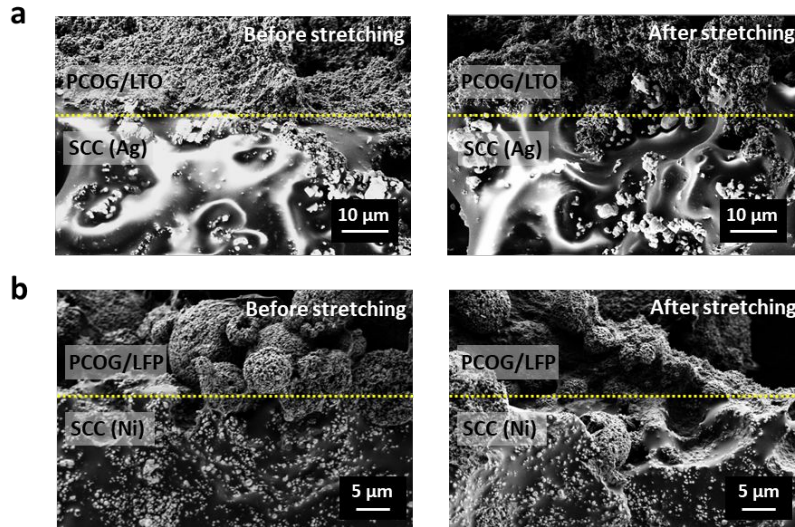


Figure S17. SEM images of the interfaces between the stretchable (a) PCOG/LTO composite anode and stretchable current collector with Ag particles and (b) PCOG/LFP composite cathode and stretchable current collector with Ni particles before and after repetitive stretching/releasing at 50% for 100 cycles.

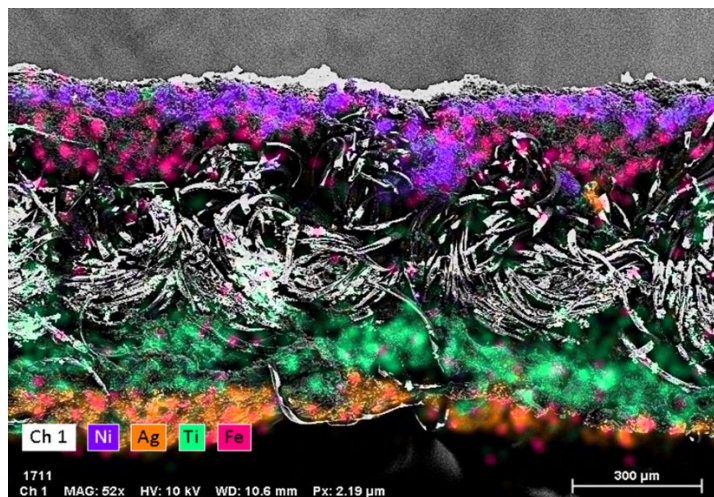


Figure S18. EDS spectrum of the cross-sectioned printed stretchable battery on stretch fabric with SCC-Ni/PCOG-LFP/stretch fabric/PCOG-LTO/SCC-Ag laminated structure.

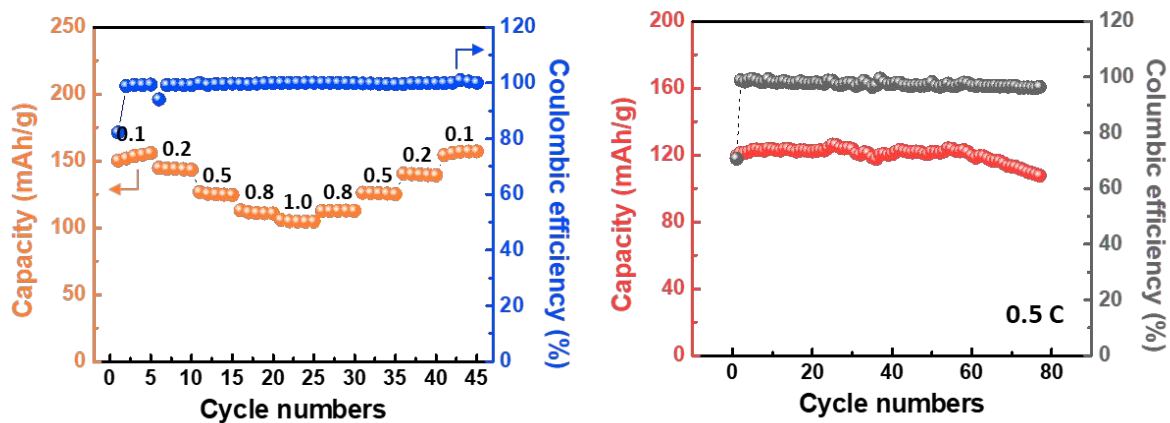


Figure S19. Rate capability, cycling performance and Coulombic efficiency of fabric-based stretchable LIB.

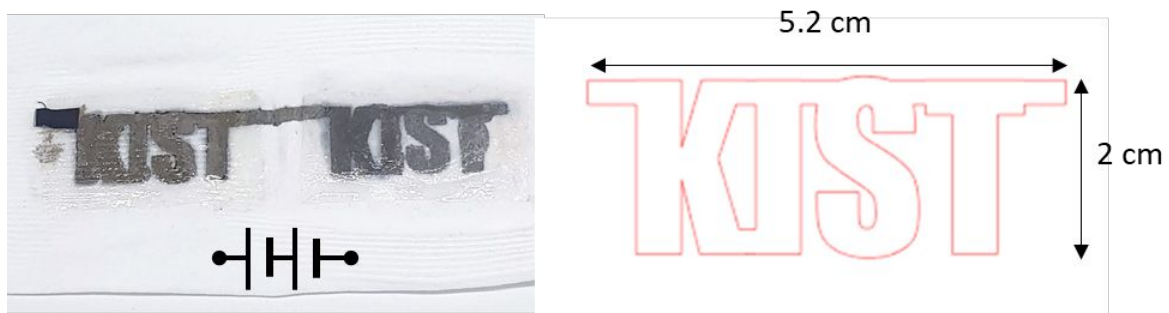


Figure S20. Photographic image of 2 series printed stretchable LIB with our institute name onto stretch fabric and dimensions of electrode pattern.

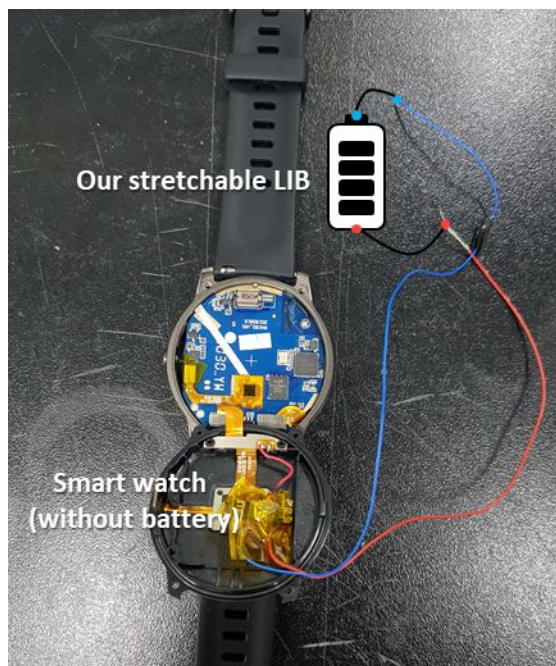


Figure S21. Photographic image of disassembled smart watch without commercial battery.

	Stretchable approach	Electrode Materials			Electrolyte	Encapsulant	Capacity of stretchable electrodes	Operation voltage	Energy density	Strain stability (C/C ₀)	Repetitive strain stability (C/C ₀)	Long-term stability (C/C ₀)
		Cathode	Anode	Current collector								
Our work	Intrinsic	LFP /PCOG	LTO /PCOG	Stretchable Ag/Ni particle /PIB composite	1 M LiPF ₆ with PCOG (liquid+gel)	PIB	128 mAh g ⁻¹ 1.5 mAh cm ⁻² @ 0.5 C	1.8 V	2.3 mWh cm ⁻² 57.5 mWh cm ⁻³	0.94 @50%, 0.5 C	0.89 @1000 times, 50%, 0.5 C	0.92 @110 cycles, 0.5 C in air
	(on stretch fabric)											
	(high voltage)		142 mAh g ⁻¹ @ 0.5 C				3.2 – 3.35 V	2.6 mWh cm ⁻²	0.93 @2 mm bending radius, 0.5 C	-	-	
[1]	Intrinsic	LFP /SLIC	LTO /SLIC	Au/SLIC	LiTFSI/SLIC	PDMS	~50 mAh g ⁻¹ @ 0.5 C 108 mAh g ⁻¹ , 1.1 mAh cm ⁻² @ 0.1 C	1.7 – 1.8 V	-	0.92 @ 70%, 0.1 C	0.89 @ 10 times, 50%	N/R
[2]	Wavy current collector & Sticky separator	LCO	Graphite	Al/Cu foils*	1 M LiPF ₆ (liquid)	PDMS	2.2 mAh cm ⁻² @ 0.5 C	3.6 V	110 mWh cm ⁻³	0.91 @ 50%	No repetitive strain test	0.85 @ 60 cycles, 0.5 C
[3]	Pre-strain Wavy (450%)	LMO/PDMS** (~40%)	LTO/PDMS** (~40%)	N/A	LiTFSI/PEO (gel)	PDMS	0.12 mAh cm ⁻² @ 1 C	1.55 V	1.6 mWh cm ⁻²	0.97 @ 400%	0.97 @200 times, 400%	0.87 @ 100 cycles, 1 C
[4]	Porous PDMS	LFP/CNT /PDMS**	LTO/CNT /PDMS**	N/A	1 M LiPF ₆ PVDF-HFP (liquid+gel)	PDMS	0.64 mAh cm ⁻² @ 0.532 C	1.7 V	-	0.88 @ 50% 0.075 C	0.84 @100 times, 50% 0.075 C	N/R
[5]	Rigid Islands on Ecoflex	LCO	LTO	Al/Cu*	LiClO ₄ /PEO (gel)	Ecoflex	1.1 mAh cm ⁻² @ 0.5 C (areal coverage 33% (catho), 17% (ano))	2.3 V	-	~1 @ 300%	N/R	~0.75 @ 20 cycles
[6]	Wire	LMO/CNT	LTO/CNT	N/A	LiTFSI/PEO (gel)	Heat-shrinkable tube	138 mAh g ⁻¹ 0.0028 mAh cm ⁻¹ @ 0.01 mA	2.2 V	17.7 mWh cm ⁻³	0.8 @ 100%	0.9 @ 200 times, 100%	0.85 @ 100 cycles, 0.05 mA
[7] our previous	Reentrant 2D cellular	LFP/CN T-rGO	LTO/CN T-rGO	N/A	1 M LiPF ₆ PVDF-HFP (liquid+gel)	Butyl rubber	140 mAh g ⁻¹ @ 0.5 C, 5.05 mAh cm ⁻² @0.2 C	1.8 V	102.4 mWh g ⁻¹	0.94 @ 50%, 3 C	0.93 @500 times, 50%	0.957 @100 cycles, 3 C

Table S1. Comparison of our all-component intrinsically stretchable battery with other non-aqueous stretchable lithium-ion batteries reported in previous research. *non-stretchable, **non-participant for energy storage, N/A = not applicable, N/R = not rated.

References

- [1] Mackanic, D. G.; Yan, X.; Zhang, Q.; Matsuhisa, N.; Yu, Z.; Jiang, Y.; Manika, T.; Lopez, J.; Yan, H.; Liu, K.; Chen, X.; Cui, Y.; Bao, Z., Decoupling of Mechanical Properties and Ionic Conductivity in Supramolecular Lithium Ion Conductors. *Nat. Commun.* **2019**, *10* (1), 5384.
- [2] Liu, W.; Chen, J.; Chen, Z.; Liu, K.; Zhou, G.; Sun, Y.; Song, M.-S.; Bao, Z.; Cui, Y., Stretchable Lithium-Ion Batteries Enabled by Device-Scaled Wavy Structure and Elastic-Sticky Separator. *Adv. Energy Mater.* **2017**, *7* (21), 1701076.
- [3] Weng, W.; Sun, Q.; Zhang, Y.; He, S.; Wu, Q.; Deng, J.; Fang, X.; Guan, G.; Ren, J.; Peng, H., A Gum-Like Lithium-Ion Battery Based on a Novel Arched Structure. *Adv. Mater.* **2015**, *27* (8), 1363-1369.
- [4] Liang, J.; Wang, S.; Yu, H.; Zhao, X.; Wang, H.; Tong, Y.; Tang, Q.; Liu, Y., Solution-Processed PDMS/SWCNT Porous Electrodes with High Mass Loading: toward High Performance All-Stretchable-Component Lithium Ion Batteries. *Sustain. Energy Fuels* **2020**, *4*, 2718.
- [5] Xu, S.; Zhang, Y.; Cho, J.; Lee, J.; Huang, X.; Jia, L.; Fan, J. A.; Su, Y.; Su, J.; Zhang, H.; Cheng, H.; Lu, B.; Yu, C.; Chuang, C.; Kim, T.-i.; Song, T.; Shigeta, K.; Kang, S.; Dagdeviren, C.; Petrov, I. *et al.*, Stretchable Batteries with Self-Similar Serpentine Interconnects and Integrated Wireless Recharging Systems. *Nat. Commun.* **2013**, *4*, 1543.
- [6] Ren, J.; Zhang, Y.; Bai, W.; Chen, X.; Zhang, Z.; Fang, X.; Weng, W.; Wang, Y.; Peng, H., Elastic and Wearable Wire-Shaped Lithium-Ion Battery with High Electrochemical Performance. *Angew. Chem.* **2014**, *126* (30), 7998-8003.

[7] Kang, S.; Hong, S. Y.; Kim, N.; Oh, J.; Park, M.; Chung, K. Y.; Lee, S.-S.; Lee, J.; Son, J. G., Stretchable Lithium-Ion Battery Based on Re-Entrant Micro-Honeycomb Electrodes and Cross-Linked Gel Electrolyte. *ACS Nano* **2020**, *14* (3), 3660-3668.